

Ortho substituted 1,3,5-Triphenylbenzene hole transport materials for perovskite solar cells

Michal Maciejczyk^a, Ruihao Chen^b, Alasdair Brown^a, Nanfeng Zheng^{b*} and Neil Robertson^{a*}

^a School of Chemistry and EaStCHEM, University of Edinburgh, King's Buildings, David Brewster Road, Edinburgh, Scotland EH93FJ, UK. E-mail: Neil.Robertson@ed.ac.uk

^b State Key Laboratory of Physical Chemistry of Solid Surfaces, Xiamen University, 422 Siming South Road, Xiamen, Fujian 361005, P. R. China, Email: nfzheng@xmu.edu.cn

Table of contents

Experimental Section.....	2
General methods	2
Electrochemistry	2
UV-Visible Spectroscopy	4
Thermal Analysis	4
Powder X-Ray Diffraction.....	6
Cost analysis	7
Synthesis	7
Solubility.....	9
Device performance.....	9
NMR Spectra	12

Experimental Section

General methods

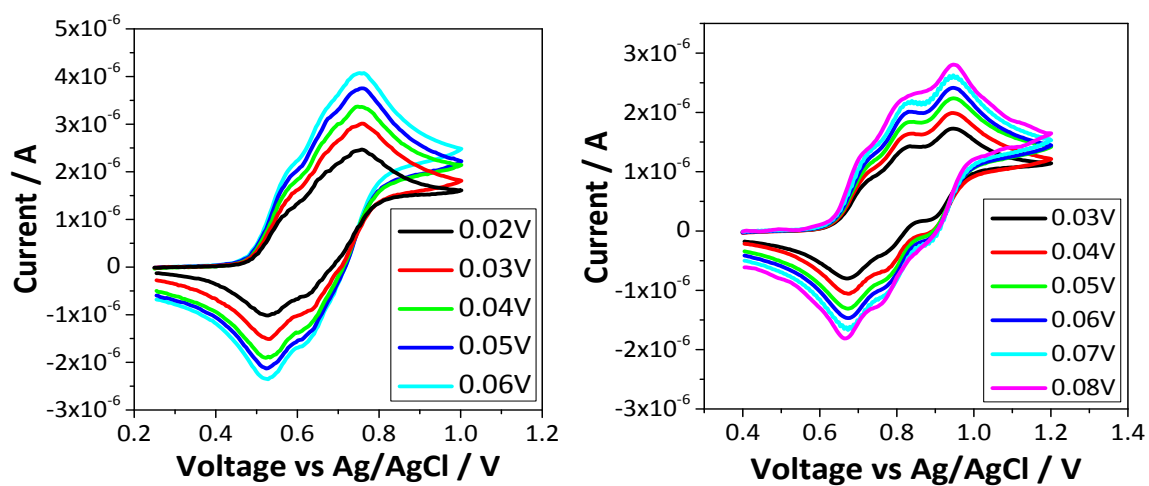
Elemental analyses were carried out by Stephen Boyer of the Science Centre, London Metropolitan University using a Carlo Erba CE1108 Elemental Analyser. NMR spectroscopy was conducted using Bruker (400, 500 or 600 MHz) spectrometers. ^1H and ^{13}C NMR spectra were all recorded in deuterated dichloromethane. Mass spectra were recorded with Xevo QTOF (Waters) high resolution, accurate mass tandem mass spectrometer equipped with Atmospheric Solids Analysis Probe (ASAP) and Bruker MicroToF 2. All spectra were recorded using electrospray ionisation (ESI).

FTO glass substrates were sequentially washed in ultrasonic baths of detergent, acetone, distilled water and ethanol for 10 min, respectively. Then, The FTO was calcined at 500 °C for 0.5 h. The ZnO layer was firstly deposited on the FTO. The precursor solution of magnesium acetate tetrahydrate (169 mg) and 8 mg ethanolamine (EA) in 2.3 mL of anhydrous ethanol was spin-coated on pre-treated ZnO substrate. The substrate was then annealed at 450 °C for 30 min to obtain the ZnO-MgO-EA (NH_3)⁺ ETL. A 150 nm thick layer of mesoporous-TiO₂ was deposited on the ZnO-MgO-EA (NH_3)⁺ substrate by spin-coating of the TiO₂ paste (Dyesol DSL 18NR-T) with ethanol (1:5, mass ratio), which was followed by annealing at 450 for 30 min. The CH₃NH₃PbI₃ perovskite layers were fabricated by reacting mesoporous PbI₂ (m-PbI₂) with CH₃NH₃I. A mixture of 461 mg of PbI₂ and 70 mg of dimethyl sulfoxide (DMSO) dissolved in 600 mg of N,N-Dimethylformamide (DMF) was spin-coated on the as-prepared substrate at 3,000 rpm for 25 s. The films were annealed at 70 °C for 15 min to obtain the m-PbI₂ film. After cooling to room temperature, the m-PbI₂ film was immersed into the solution of CH₃NH₃I in isopropanol for 45 s, and then was washed by isopropanol to remove the excess I-rich ionic compound. After the preparation of perovskite layer, different hole transport layers were coated via solution process at 4,000 rpm for 30 s, with the additives containing Li-TFSI/acetonitrile and TBP. Finally, an 80-nm thick Au counter electrode was deposited via thermal evaporation under reduced pressure of 4×10^{-7} Torr. The active area was 0.10 cm².

Electrochemistry

All cyclic voltammetry measurements were carried out in freshly distilled CH₂Cl₂ using 0.3 M [TBA][PF₆] electrolyte in a three-electrode system, with each solution being purged with N₂ prior to measurement. The working electrode was a Pt disk (0.2 mm). The reference electrode was Ag/AgCl and the counter electrode was a Pt rod. All measurements were made at room temperature using a mAUTOLAB Type III potentiostat, driven by the electrochemical software GPES. Cyclic voltammetry (CV) measurements used scan rates of 0.05 V s⁻¹. Square wave voltammetry (SWV) was carried out at a step potential of 0.004 V, square wave amplitude of 0.025 V, and a square wave frequency of 25 Hz. Ferrocene was used as the internal standard in each measurement.

Figure S1. Cyclic voltammograms at different scan rates for TPB(2-MeOTAD) (left) and TPB(2-TPTZ) (right).



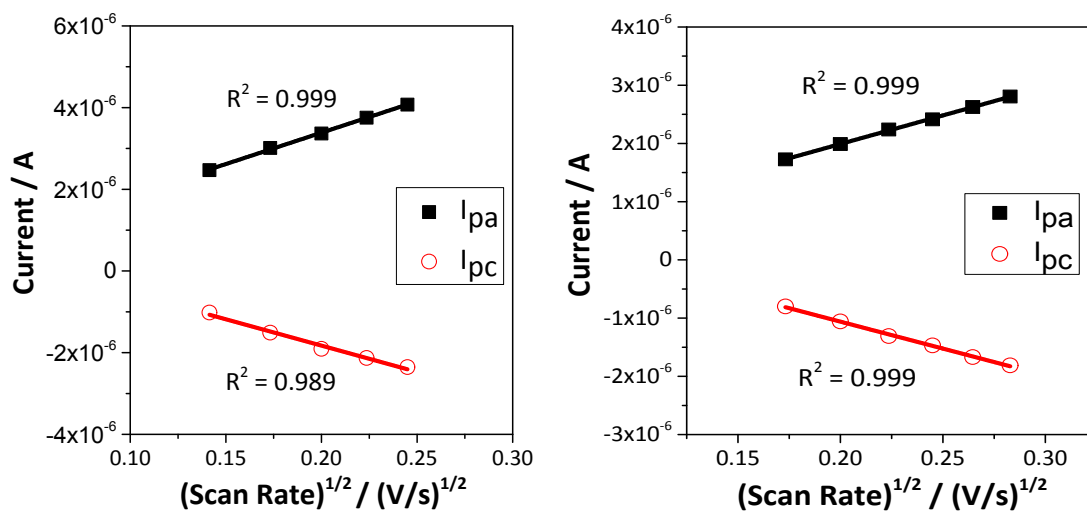


Figure S2. Plots of peak anodic (I_{pa}) and cathodic (I_{pc}) currents against the square root of the scan rate for TPB(2-MeOTAD) (left) and TPB(2-TPTZ) (right).

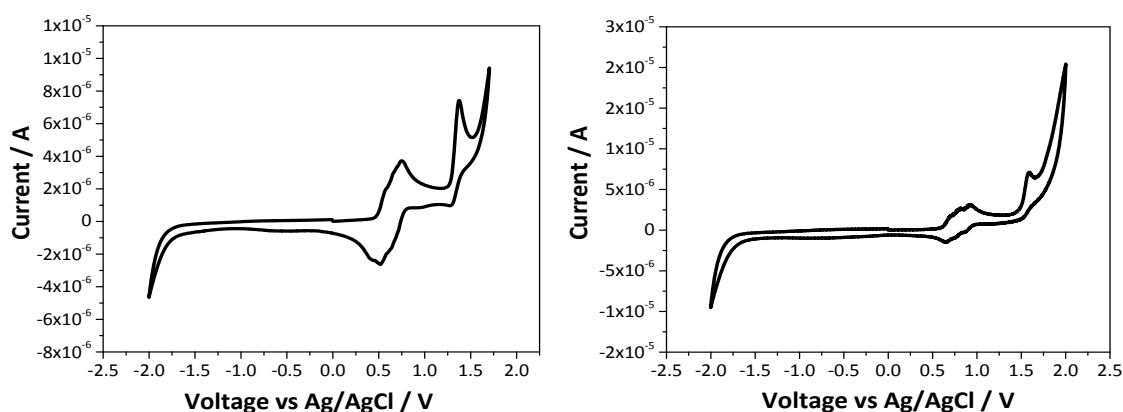


Figure S3. Full cyclic voltammograms for TPB(2-MeOTAD) (left) and TPB(2-TPTZ) (right).

Table S1. Half wave potentials for each oxidation peak from cyclic voltammetry measurements.

Material	$E_{1/2}$ (1) / V	$E_{1/2}$ (2) / V	$E_{1/2}$ (3) / V	$E_{1/2}$ (4) / V
TPB(2-MeOTAD)	0.19	0.29	0.36	0.99 [†]
TPB(2-TPTZ)	0.24	0.33	0.44	1.11 [†]

[†]Chemically irreversible

UV-Visible Spectroscopy

UV-visible absorption spectra were recorded in solution using a Jasco V-670 UV/vis/NIR spectrophotometer controlled with SpectraManager software. All samples were measured at a concentration of 2×10^{-5} M in dichloromethane, at room temperature in a 1 cm cell.

Thermal Analysis

Differential scanning calorimetry (DSC) and Thermal Gravimetric Analysis were performed on NETZSCH STA 449F1 at scan rates of 20 and 10 K min⁻¹ under nitrogen atmosphere in DSC/TG aluminium pan. The measurement range was 25 °C to 350 °C.

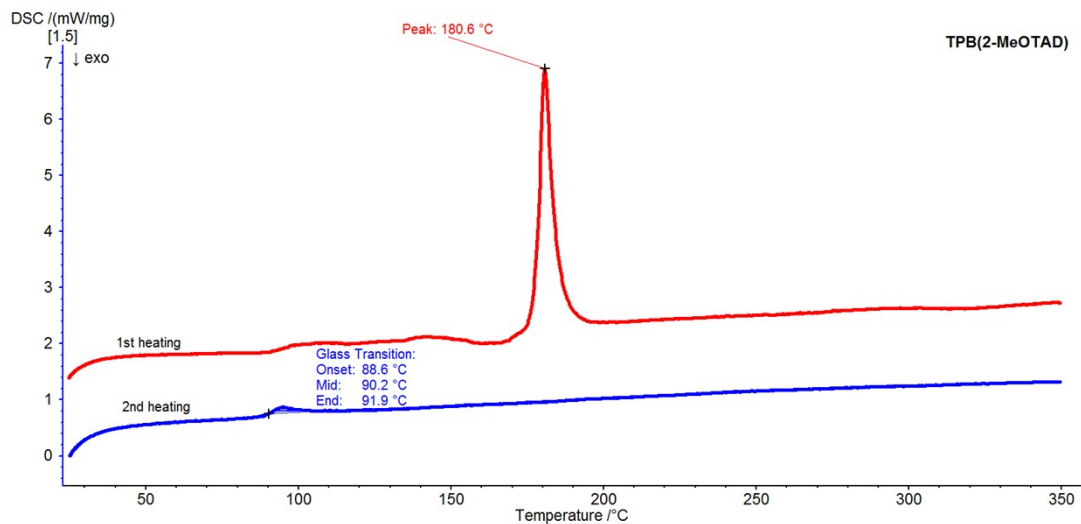


Figure S4. Differential Scanning Calorimetry for TPB(2-MeOTAD), measured at 20 K min⁻¹.

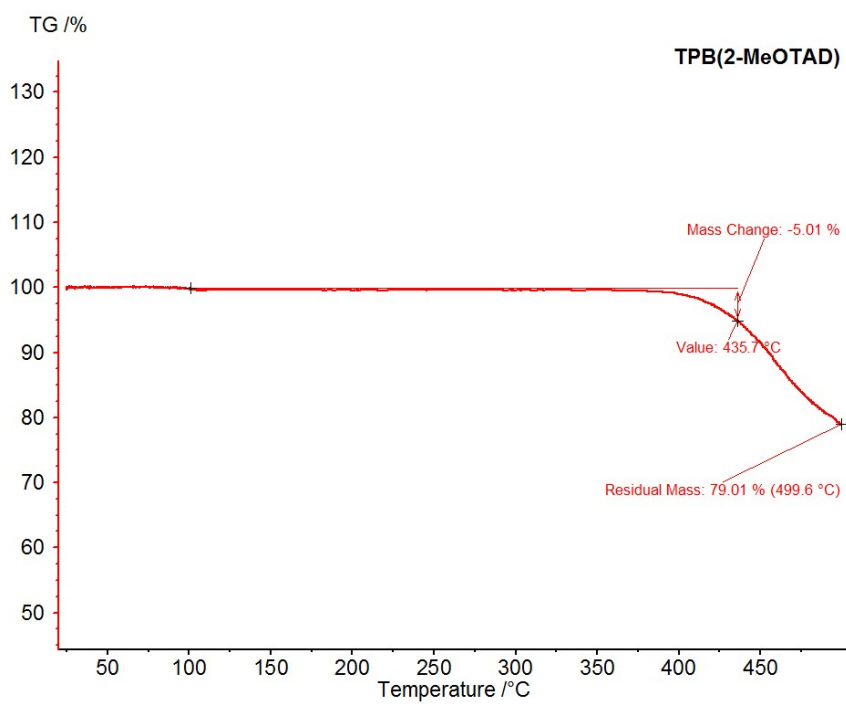


Figure S5. Thermal Gravimetric Analysis of TPB(2-MeOTAD), measured at 10 K min⁻¹.

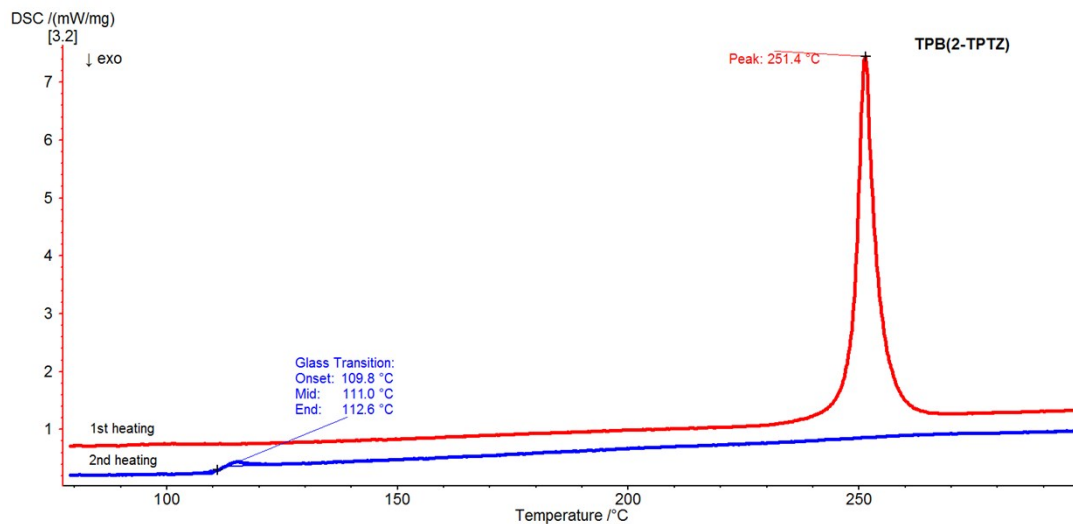


Figure S6. Differential Scanning Calorimetry for TPB(2-TPTZ), measured at 25 K min⁻¹.

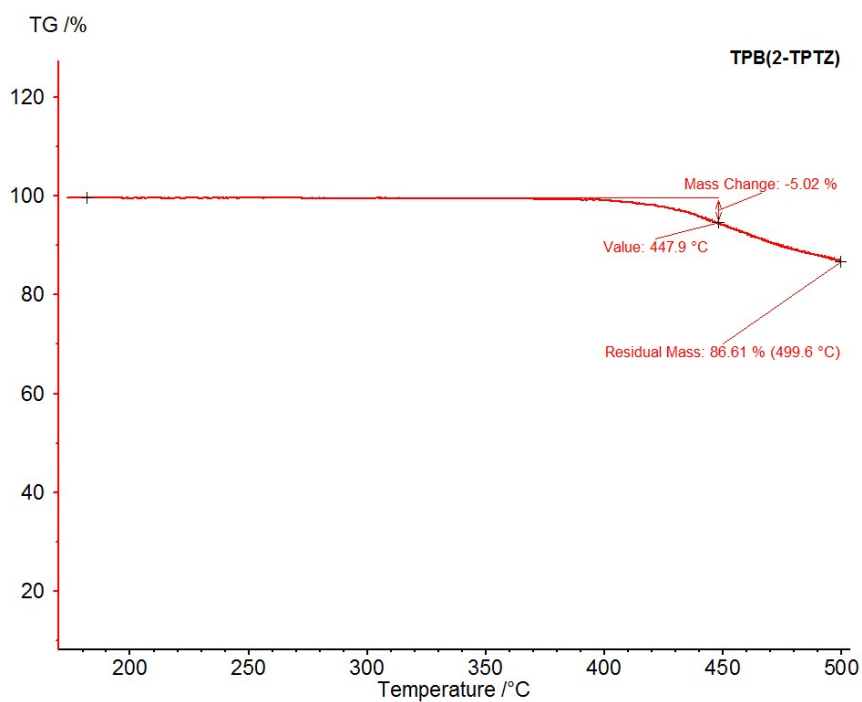


Figure S5. Thermal Gravimetric Analysis of TPB(2-TPTZ), measured at 10 K min⁻¹.

Powder X-Ray Diffraction

Powder diffraction was performed on a Bruker Discover D8 with CuK_{a1/2} source and a scintillation detector.

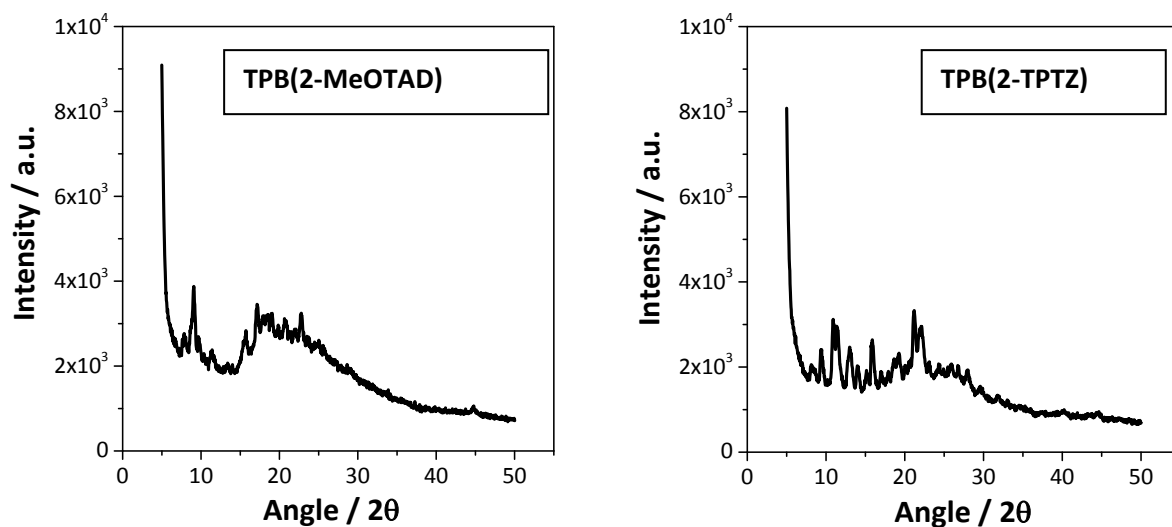


Figure S8. Powder X-Ray Diffraction data for TPB(2-MeOTAD) and TPB(2-TPTZ).

Cost analysis

We conducted simplified cost analysis of the studied materials. We did not include workup/purification steps as this is highly variable and can be optimized to reduce final cost of the step. Especially typically used solvents like dichloromethane/chloroform or method of purification like column chromatograph, constituting significant percentage of the final cost, on the large scale would be substituted by appropriate solvent choice and more cost efficient purification method like crystallization.

Table S2. Materials quantities and cost for the synthesis of TPB(2-TBr).

Chemical name	Weight reagent (g/g)	Price of Chemical (\$/g)	Material Cost (\$/g product)	Percentage of Step (%)
2'-Bromoacetophenone	1.134	0.96	1.09	66.2
SiCl ₄	2.895	0.12	0.35	21.1
Ethanol	6.919	0.03	0.21	12.6
Total cost (\$/g)			1.64	

Table S3. Materials quantities and cost for the synthesis of TPB(2-MeOTAD).

Chemical name	Weight reagent (g/g)	Price of Chemical (\$/g)	Material Cost (\$/g product)	Percentage of Step (%)
TPBBr	0.758	1.64	1.24	9.6
Dimethoxydiphenylamine	1.288	8.6	11.08	85.3
Pd(OAc) ₂	0.011	19.45	0.21	1.6
P(t-Bu) ₃ HBF ₄	0.015	6.72	0.10	0.8
Toluene	10.404	0.03	0.31	2.4
NaOt-Bu	0.682	0.05	0.03	0.3
Total cost (\$/g)			12.98	

Table S4. Materials quantities and cost for the synthesis of TPB(2-TPTZ).

Chemical name	Weight reagent (g/g)	Price of Chemical (\$/g)	Material Cost (\$/g product)	Percentage of Step (%)
TPBBr	1.214	1.64	1.99	64.4
Phenothiazine	1.781	0.025	0.04	1.4
Pd(OAc) ₂	0.01	19.45	0.19	6.3
P(t-Bu) ₃ HBF ₄	0.026	6.72	0.17	5.6
Toluene	20.808	0.03	0.62	20.2
NaOt-Bu	1.288	0.05	0.06	2.1
Total cost (\$/g)			3.09	

For the cost-per-peak-Watt estimation we assumed 200 nm thick HTM layer and no loss of the hole transporting material during processing, following method introduced by Osedach *et al.* and further developed by Petrus *et al.*^{1,2,3} Assumed price for spiro-MeOTAD was 100 \$/g while prices of TPB(2-MeOTAD) and TPB(2-TPTZ) were taken from cost estimation shown in tables above showing 12.98 \$/g and 3.09 \$/g, respectively.

Synthesis

All preparations were carried out using standard Schlenk line and air-sensitive chemistry techniques under nitrogen atmosphere. The starting material, 1,3,5-Tris(2-bromophenyl) benzene has been prepared according to previously reported procedure.⁴ All other materials were purchased from

¹ T. P. Osedach, T. L. Andrew and V. Bulović, *Energy Environ. Sci.*, 2013, **6**, 711.

² M. L. Petrus, M. T. Sirtl, A. C. Closs, T. Bein and P. Docampo, *Mol. Syst. Des. Eng.*, 2018, **3**, 734–740.

³ M. L. Petrus, T. Bein, T. J. Dingemans and P. Docampo, *J. Mater. Chem. A*, 2015, **3**, 12159–12162.

⁴ I. D. Trawny, M. Quennet, N. Rades, D. Lentz, B. Paulus and H.-U. Reissig, *European J. Org. Chem.*, 2015, **2015**, 4667–4674.

commercial suppliers and used without further purification. Toluene was dried using a solvent purification system. Column chromatography was carried out using Silica 60A (particle size 35-70 μm , Fisher, UK) as the stationary phase, and TLC was performed on pre-coated silica gel plates (0.25 mm thick, 60 F254, Merck, Germany) and observed under UV light.

1,3,5-Tris(2'-((N,N-di(4-methoxyphenyl)amino)phenyl)benzene (TPB(2-MeOTAD))

A mixture of 1,3,5-Tris(2-bromophenyl) benzene (0.50 g, 0.921 mmol), 4,4'-dimethoxydiphenylamine (0.85 g, 3.707 mmol), palladium (II) acetate (0.007 g, 0.031 mmol), sodium *tert*-butoxide (0.45 g, 4.683 mmol) and tri-*tert*-butylphosphonium tetrafluoroborate (0.01 g, 0.034 mmol) was added to an oven-dried Schlenk tube and dried under vacuum for 30 minutes. Dry toluene (12 mL) was added and the mixture was stirred under nitrogen at 110 °C for 24 hours. The solution was diluted with dichloromethane, filtered through Cellite, washed with acetone and concentrated on a rotary evaporator. The residue was purified by column chromatography (SiO_2 , eluent: 5:1 acetone:hexane) then precipitated from a solution of acetone into an excess of methanol. The precipitate was filtered off and washed with methanol. The white solid was dried under vacuum for 2 hours. This reaction was conducted twice to collect at least 1 g of material. The first and second reactions yielded 0.66 g (73%) and 0.49 g (55%) respectively.

Elemental Analysis (%). Calculated for $\text{C}_{66}\text{H}_{57}\text{N}_3\text{O}_6$: C 80.08, H 5.74, N 4.34. Found: C 80.13, H 5.74, N 4.36.

^1H NMR (500 MHz, Methylene Chloride- d_2) δ 3.70 (s, 18H), 6.56 (d, 24H), 6.63 (s, 3H), 6.87 (d, $J = 7.5$ Hz, 3H), 7.10 (d, $J = 7.8$ Hz, 3H), 7.15 (t, $J = 7.3$ Hz, 3H), 7.27 (t, $J = 7.9$ Hz, 3H).

^{13}C NMR (126 MHz, Methylene Chloride- d_2) δ 53.0, 53.2, 53.4, 53.6, 53.8, 55.3, 113.9, 123.5, 124.5, 127.4, 128.3, 128.4, 131.9, 139.0, 140.6, 142.0, 145.7, 154.3.

MS (ESI): m/z (%) = 988.4 [(M + H) $^+$, 100].

1,3,5-Tris(2'-((N-phenothiazyl)phenyl)benzene (TPB(2-TPTZ))

A mixture of 1,3,5-Tris(2-bromophenyl) benzene (0.50 g, 0.921 mmol), phenothiazine (0.80 g, 4.015 mmol), palladium (II) acetate (0.006 g, 0.027 mmol), sodium *tert*-butoxide (0.48 g, 4.995 mmol) and tri-*tert*-butylphosphonium tetrafluoroborate (0.018 g, 0.062 mmol) was added to an oven-dried Schlenk tube and dried under vacuum for 30 minutes. Dry toluene (12 mL) was added and the mixture was stirred under nitrogen at 110 °C for 24 hours. The solution was diluted with dichloromethane, filtered through Cellite, washed with acetone and concentrated on a rotary evaporator. The residue was purified by column chromatography (SiO_2 , eluent: 85:10:5 petroleum ether (40-60):chloroform:diethyl ether) then precipitated from a solution of acetone into an excess of methanol. The precipitate was filtered off

and washed with methanol. The white solid was dried under vacuum for 2 hours. This reaction was repeated with the same proportions but on a 1.25 g scale to yield over 1 g of product. The first and second reactions yielded 0.31 g (36%) and 1.03 g (50%) respectively.

Elemental Analysis (%). Calculated for C₆₀H₃₉N₃S₃: C 80.06, H 4.39, N 4.59; Found: C 80.11, H 4.30, N 4.62.

¹H NMR (500 MHz, Methylene Chloride-d₂) δ 6.06 (d, *J* = 6.1 Hz, 6H), 6.68-6.74 (m, 12H), 6.88 (dd, *J* = 6.9, 2.3 Hz, 6H), 7.34 (d, *J* = 8.2 Hz, 3H), 7.39 (t, *J* = 7.5 Hz, 3H), 7.51 (s, 3H), 7.51-7.55 (m, 6H).

¹³C NMR (126 MHz, Methylene Chloride-d₂) δ 53.0, 53.2, 53.4, 53.6, 53.8, 115.7, 118.8, 122.1, 126.2, 126.9, 128.5, 128.8, 129.1, 132.9, 137.2, 137.4, 141.2, 143.8.

MS (ESI): *m/z* (%) = 897.2 [(M + H)⁺, 100].

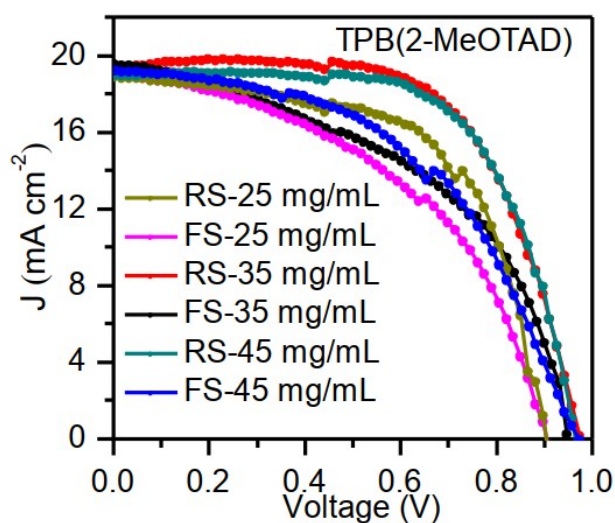
Solubility

Table S5. Solubility of HTMs.

Material	Chloroform	Toluene	Chlorobenzene
TPB(2-MeOTAD)	>100 mg/ml	>160 mg/ml	>50 mg/ml
TPB(2-TPTZ)	>260 mg/ml	>50 mg/ml	>110 mg/ml

Device performance

J-V Test TPB(2-MeOTAD)



Name	$J_{sc}/\text{mA}\cdot\text{cm}^{-2}$	V_{oc}/V	FF/%	$\eta/\%$	$R_s/\Omega\cdot\text{cm}^{-2}$
RS-25 mg/mL	18.86	0.90	60.37	10.25	10.74
FS-25 mg/mL	18.96	0.90	47.77	8.15	13.19
RS-35 mg/mL	19.32	0.97	64.54	12.14	9.10
FS-35 mg/mL	19.64	0.96	48.26	9.10	10.36
RS-45 mg/mL	18.93	0.96	66.13	12.02	8.08
FS-45 mg/mL	19.18	0.97	51.86	9.65	24.76

Figure S9. *J-V* curves and photovoltaic parameters of the devices with different concentration of TPB(2-MeOTAD) as HTM, recorded using from forward and reverse bias to short circuit.

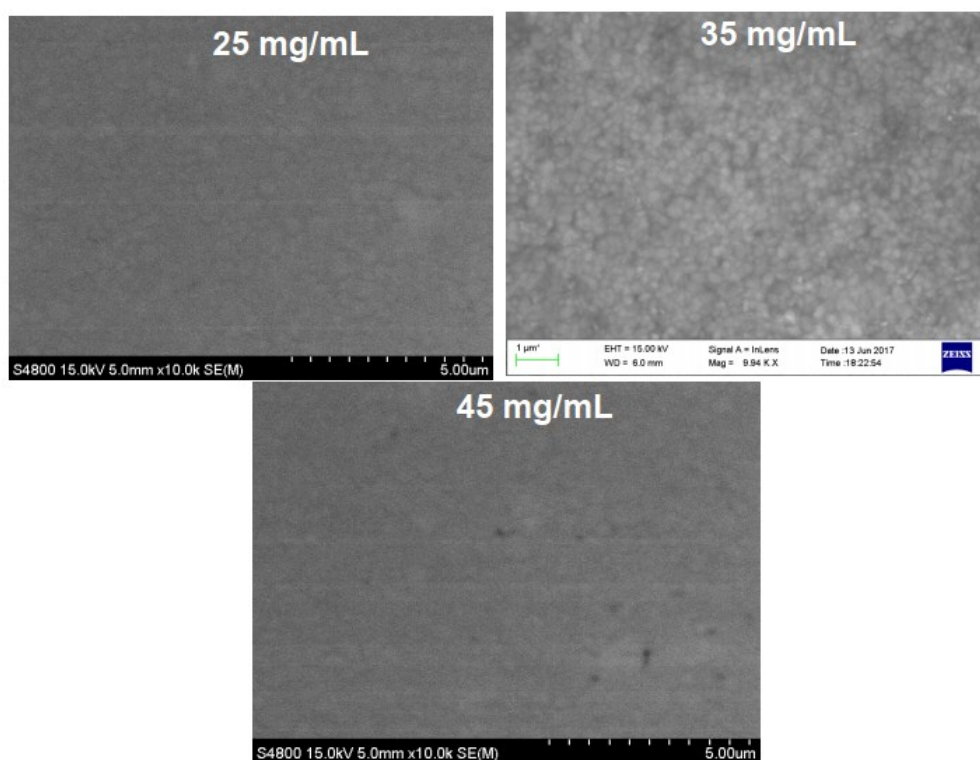
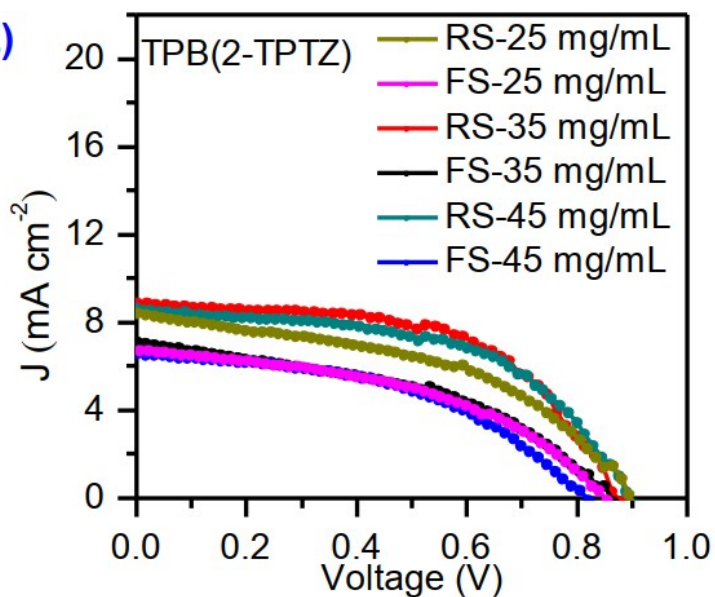


Figure S10. Top-view SEM images of PSCs with TPB(2MeOTAD) as HTM with different concentration.

J-V Test TPB(2-TPTZ)



Name	$J_{sc}/\text{mA}\cdot\text{cm}^{-2}$	V_{oc}/V	FF/%	$\eta/\%$	$R_s/\Omega\cdot\text{cm}^{-2}$
RS-25 mg/mL	8.50	0.90	46.17	3.53	29.64
FS-25 mg/mL	6.78	0.85	44.45	2.56	15.31
RS-35 mg/mL	8.89	0.88	55.30	4.32	28.71
FS-35 mg/mL	6.38	0.86	43.53	2.38	39.30
RS-45 mg/mL	8.64	0.90	52.31	4.07	21.88
FS-45 mg/mL	6.61	0.81	46.19	2.50	16.92

Figure S11. J-V curves and photovoltaic parameters of the devices with different concentration of TPB(2-TPTZ) as HTM, recorded using from forward and reverse bias to short circuit.

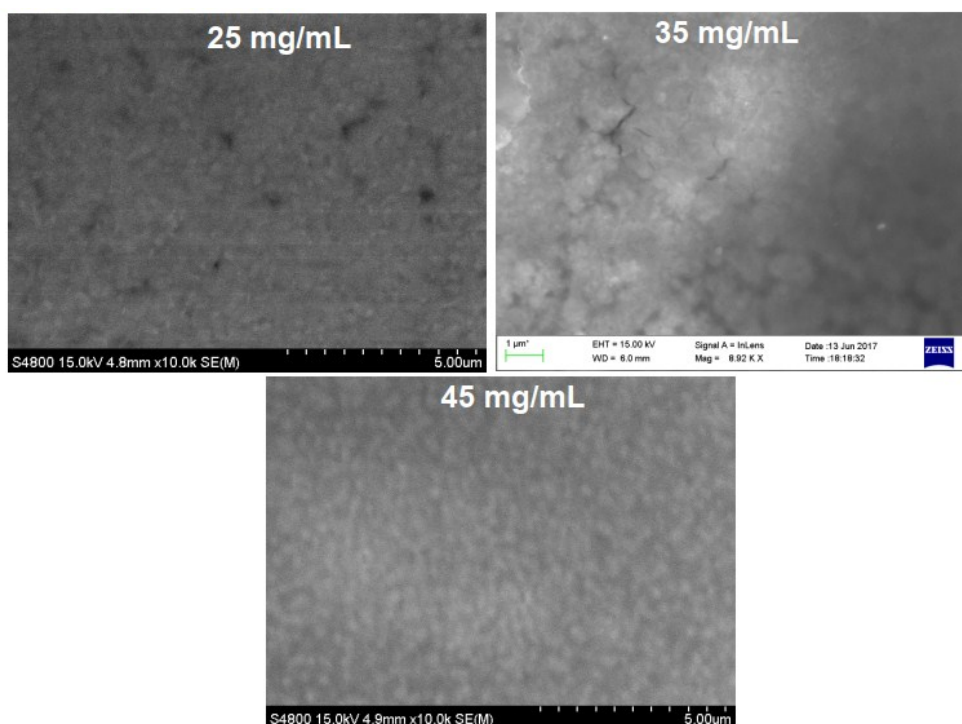


Figure S12. Top-view SEM images of PSCs with TPB(2MeOTAD) as HTM with different concentration.

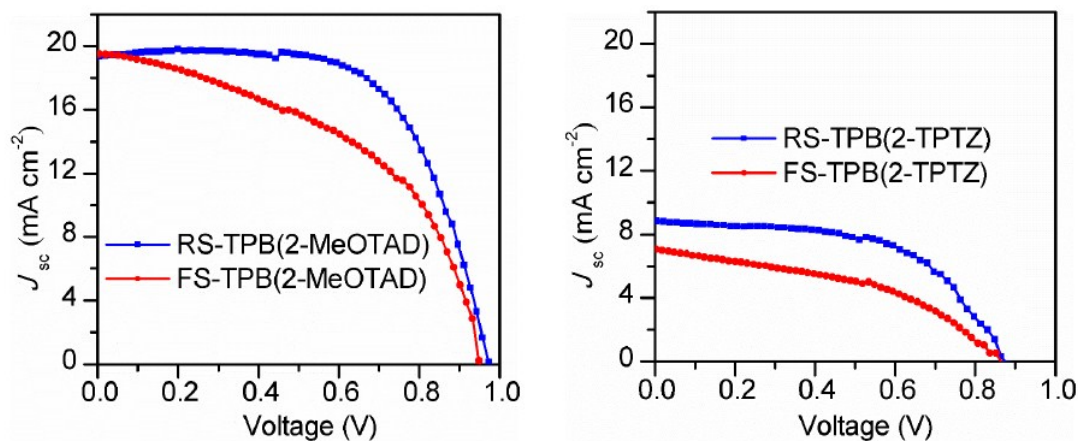


Figure S12. *J-V* curves of the champion PSCs with TPB(2-MeOTAD) and TPB(2-TPTZ) HTMs recorded using from forward and reverse bias to short circuit.

Table S6. Photovoltaic parameters determined from *J-V* measurements of PSCs based on TPB(2-MeOTAD) and TPB(2-TPTZ) as HTMs.

Name	$J_{sc}/mAcm^{-2}$	V_{oc}/V	FF/%	$\eta/\%$	$R_s/\Omega cm^{-2}$
TPB(2-MeOTAD)-RS	19.32	0.97	64.54	12.14	9.10
TPB(2-MeOTAD)-FS	19.64	0.96	48.26	9.10	10.36
TPB(2-TPTZ)-RS	8.89	0.88	55.30	4.32	28.71
TPB(2-TPTZ)-FS	6.38	0.86	43.53	2.38	39.30

RS: reverse scan, FS: forward scan.

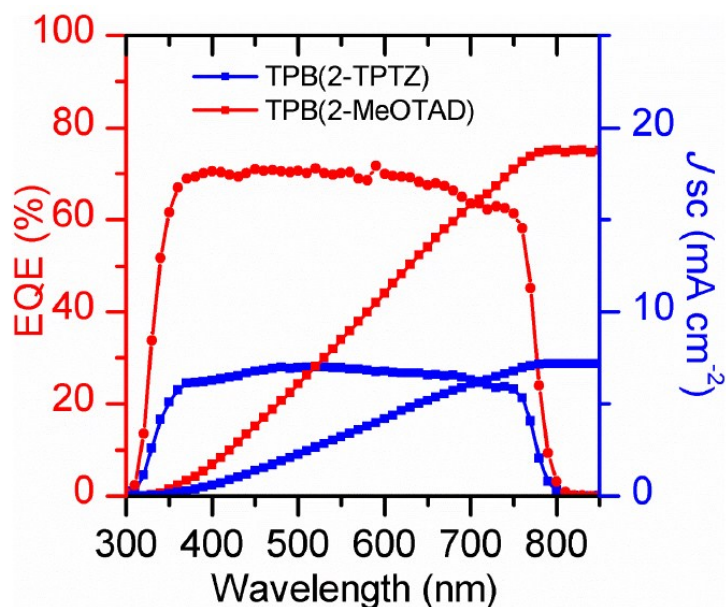


Figure S13. IPCE spectra and corresponding integrated J_{sc} of the champion devices based on TPB(2-MeOTAD) and TPB(2-TPTZ) as HTMs. Obtained values are: $18.8 mAcm^{-2}$ for TPB(2-MeOTAD) and $7.2 mAcm^{-2}$ for TPB(2-TPTZ).

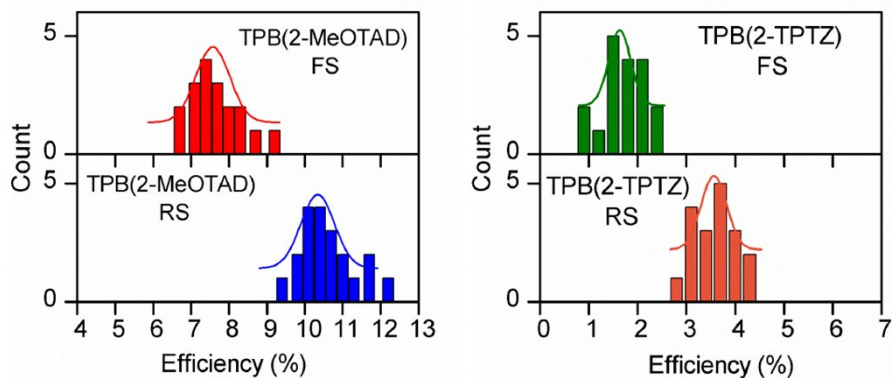


Figure S14. Devices performance statistics of 18 individual devices with TPB-2-MeOTAD and TPB(2-TPTZ) as HTM at FS and RS..

Stability

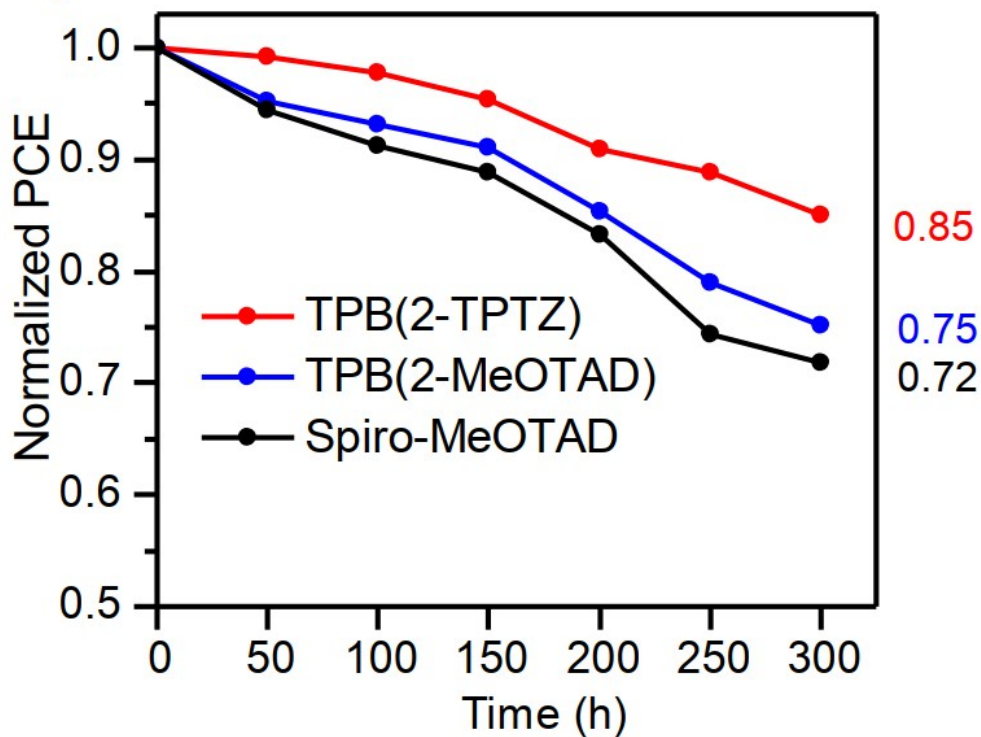


Figure S15. PCE evolution of encapsulated devices of TPB(2-MeOTAD), TPB(2-TPTZ) and Spiro-MeOTAD devices under dark storage in a dry box (25 °C, RH 30%).

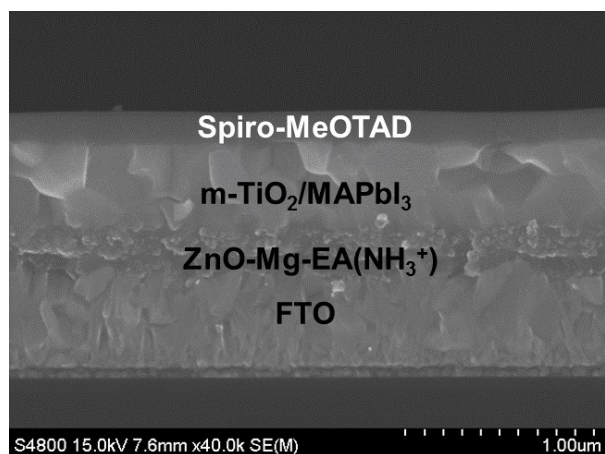
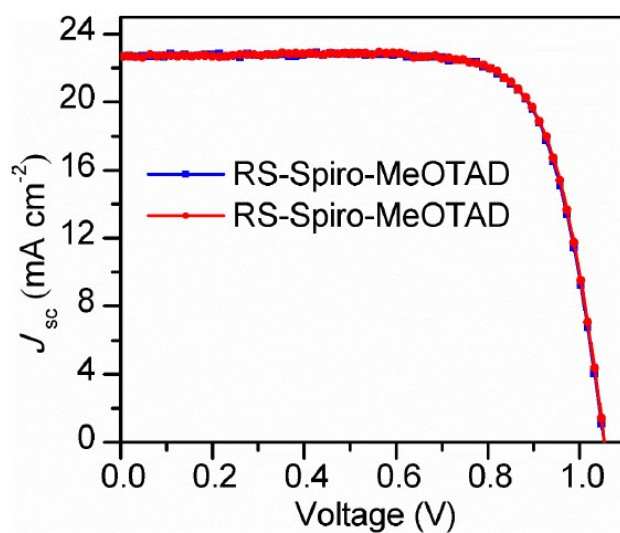


Figure S16. Cross-sectional SEM images of the control PSCs with Spiro-MeOTAD as HTM.

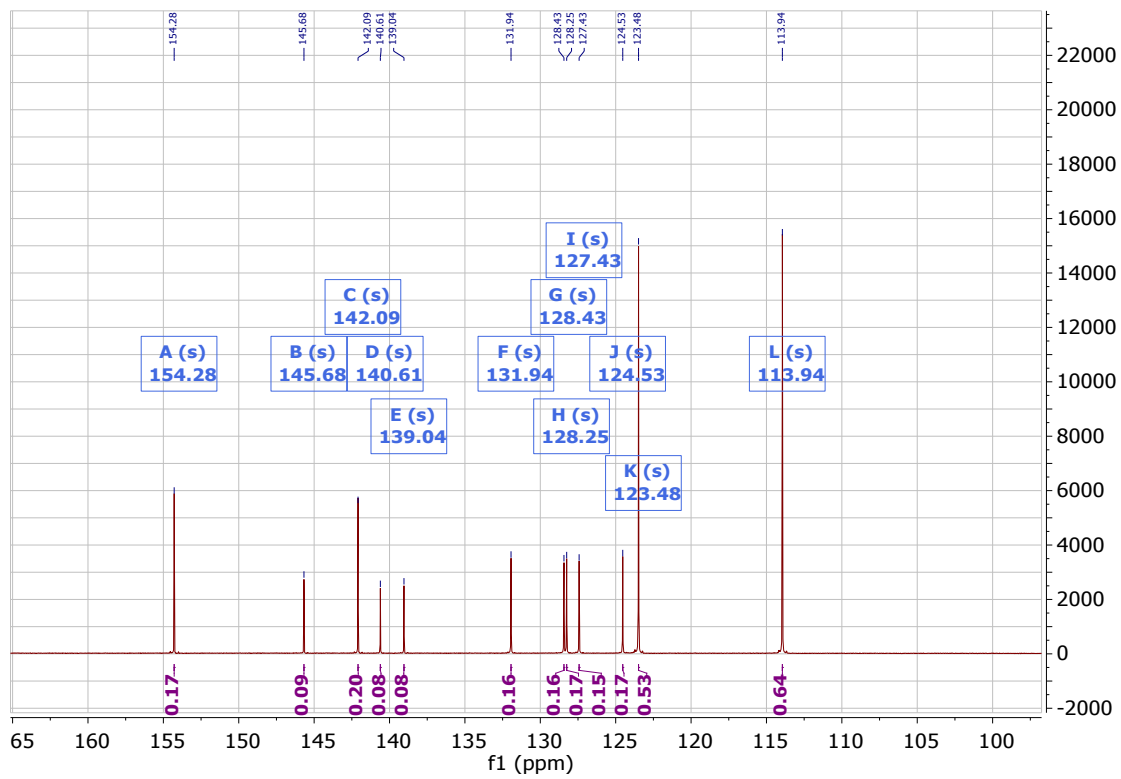
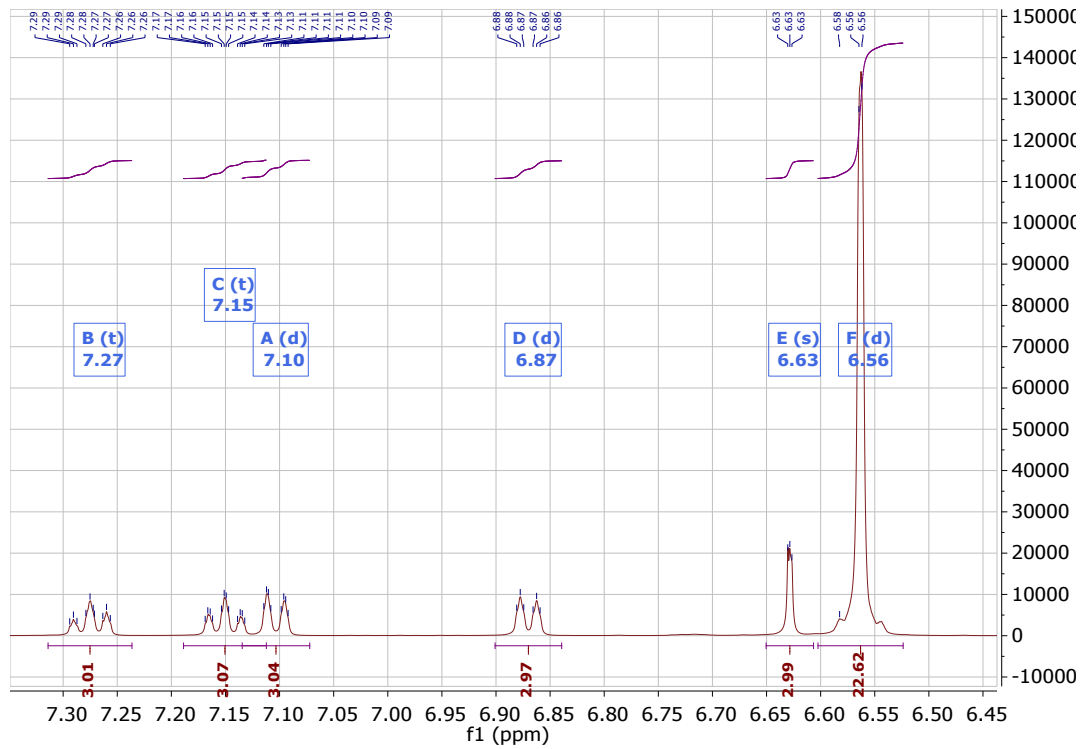


Entry	$J_{sc}/\text{mA}\cdot\text{cm}^{-2}$	V_{oc}/V	FF/%	$\eta/\%$	$R_s/\Omega\cdot\text{cm}^{-2}$
RS-Spiro-MeOTAD	22.69	1.05	75.48	18.04	4.71
FS-Spiro-MeOTAD	22.70	1.05	75.18	17.96	4.94

Figure S17. J - V curves and photovoltaic parameters of the control PSCs with Spiro-MeOTAD as HTM, recorded using from forward and reverse bias to short circuit.

NMR Spectra

TPB(2-MeOTAD)



TPB(2-TPTZ)

